Substitution Site Specificity on the $Ru_{10}C_2$ Cluster Framework. Multiple Convergent Pathways to the Mixed Hydrocarbon Ligand Derivative $Ru_{10}C_2(CO)_{21}(NBD)(C_2R_2)$

Kwangyeol Lee and John R. Shapley*

Department of Chemistry, University of Illinois, Urbana, Illinois 60801

Received July 6, 1998

The substitution of carbonyl ligands in the edge-shared bioctahedral cluster $[PPN]_2[Ru_{10}C_2(CO)_{24}]$ by two types of 4e donor π-bonding ligands, viz., a diene (norbornadiene) and an alkyne (diphenylacetylene), has been investigated under various conditions. The reaction of $[PPN]_2[Ru_{10}C_2(CO)_{24}]$ with norbornadiene (NBD) in diglyme at 140 °C has provided the anionic derivative $[PPN]_2[Ru_{10}C_2(CO)_{22}(NBD)]$ (**1**). Oxidation of this compound with $[Cp_2Fe][BF_4]$ affords the neutral derivative $Ru_{10}C_2(CO)_{23}(NBD)$ (**2**), which can also be prepared by direct oxidative substitution of $[Ru_{10}C_2(CO)_{24}]^{2-}$ with $2[Cp_2Fe][BF_4]$ in the presence of NBD. Spectroscopic and crystallographic studies of **1** and **2** show that the NBD ligand occupies a chelating position on one of the "outer" ruthenium atoms in the bifurcated $Ru_{10}C_2$ framework. This location contrasts with that adopted by the alkyne ligand in both $[PPN]_2[Ru_{10}C_2(CO)_{22}(C_2Ph_2)]$ (**3**) and $Ru_{10}C_2(CO)_{23}(C_2Ph_2)$ (**4**). In these derivatives the alkyne moiety is located in an "inner" site bridging two apical ruthenium atoms. The generality of these substitution sites was probed by preparing the mixed ligand derivative $Ru_{10}C_2(CO)_{21}(NBD)(C_2Ph_2)$ (**5**). This compound can be synthesized in four distinct ways: (1) by oxidation of **1** with $2[Cp_2Fe][BF_4]$ in the presence of C_2R_2; (2) by oxidation of **3** with $2[Cp_2Fe][BF_4]$ in the presence of NBD; (3) by substitution of two carbonyl ligands in **2** by C_2R_2 in refluxing toluene; and (4) by substitution of two carbonyl ligands in **4** by NBD in refluxing toluene. The substitution sites observed for the individual ligands are maintained in the mixed ligand derivative. The new compounds were characterized by analytical and spectroscopic methods including negative ion FAB mass spectroscopy and ^1H NMR spectroscopy as well as by X-ray crystallographic studies of compounds **2** and **5**.

Introduction

Systematic hydrocarbon ligand chemistry of higher nuclearity cluster systems is relatively underdeveloped, with most known derivatives based on the octahedral $Ru_6(\mu_6\text{-}C)$ framework.[1,2] This cluster system is sufficiently robust to allow direct thermal substitution by hydrocarbon ligands,[2i−m] but in many cases, hydrocarbon derivatives are obtained in the process of constructing the higher nuclearity cluster framework from a small cluster precursor.[2f−h] Chemical activation with the decarbonylation agent trimethylamineoxide has been used successfully in reactions involving such higher nuclearity neutral clusters as $Ru_6C(CO)_{17}$.[2a−c] However, the oxidative substitution method, which has been useful in the syntheses of several derivatives of Ru_6[3] as well as of Ir_6[4] and Re_7[5] clusters, is particularly promising for forming derivatives from stable anionic cluster compounds.

The dicarbido decaruthenium cluster $[Ru_{10}C_2(CO)_{24}]^{2-}$ has a structure that can be viewed as two Ru_6C octahedra sharing a common edge.[6] This partial fusion of subunits creates a new type of substitution site, an

(1) (a) Shriver, D. F., Kaesz, H. D., Adams, R. D., Eds. *The Chemistry of Metal Cluster Complexes*; VCH Publishers: New York, 1990. (b) Ma, L.; Williams, G. K.; Shapley, J. R. *Coord. Chem. Rev.* **1993**, *128*, 261. (c) Braga, D.; Dyson, P. J.; Grepioni, F.; Johnson, B. F. G. *Chem. Rev.* **1994**, *94*, 1587. (d) Dyson, P. J.; Johnson, B. F. G.; Martin, C. M. *Coord. Chem. Rev.* **1996**, *155*, 69.

(2) (a) Mallors, R. L.; Blake, A. J.; Parsons, S.; Johnson, B. F. G.; Dyson, P. J.; Braga, D.; Grepioni, F.; Parisini, E. *J. Organomet. Chem.* **1997**, *532*, 133. (b) Blake, A. J.; Haggitt, J. L.; Johnson, B. F. G.; Parsons, S. *J. Chem. Soc., Dalton Trans.* **1997**, 991. (c) Mallors, R. L.; Blake, A. J.; Dyson, P. J.; Johnson, B. F. G.; Parsons, S. *Organometallics* **1997**, *16*, 1668. (d) Brown, D. B.; Dyson, P. J.; Johnson, B. F. G.; Martin, C. M.; Parker, D. G.; Parsons, S. *J. Chem. Soc., Dalton Trans.* **1997**, 1909. (e) Brown, D. B.; Johnson, B. F. G.; Martin, C. M.; Parsons, S. *J. Organomet. Chem.* **1997**, *536*, 285. (f) Johnson, B. F. G.; Matters, J. M.; Gaede, P. E.; Ingham, S. L.; Choi, N.; McPartlin, M.; Pearsall, M. A. *J. Chem. Soc., Dalton Trans.* **1997**, 3251. (g) Johnson, B. F. G.; Shephard, D. S.; Braga, D.; Grepioni, F.; Parsons, S. *J. Chem. Soc., Dalton Trans.* **1997**, 3563. (h) Johnson, B. F. G.; Shephard, D. S.; Braga, D.; Grepioni, F.; Parsons, S. *J. Chem. Soc., Dalton Trans.* **1998**, 311. (i) Braga, D.; Grepioni, F.; Scaccionoce, L.; Johnson, B. F. G. *J. Chem. Soc., Dalton Trans.* **1998**, 1321. (j) Adams, R. D.; Wu, W. *Organometallics* **1993**, *12*, 1238. (k) Adams, R. D.; Wu, W. *Organometallics* **1993**, *12*, 1243. (l) Lee, K.; Hsu, H.-F.; Shapley, J. R. *Organometallics* **1997**, *16*, 3876. (m) Hsu, H.-F.; Wilson, S. R.; Shapley, J. R. *Organometallics* **1997**, *16*, 4937.

(3) Drake, S. R.; Johnson, B. F. G.; Lewis, J.; Conole, G.; McPartlin, M. *J. Chem. Soc., Dalton Trans.* **1990**, 995.

(4) Ceriotti, A.; Della Pergola, R.; Demartin, F.; Garlaschelli, L.; Manassero, M.; Masciocchi, N. *Organometallics* **1992**, *11*, 756.

(5) Hsu, G.; Wilson, S. R.; Shapley, J. R. *Organometallics* **1994**, *13*, 4159.

(6) (a) Hayward, C.-M. T.; Shapley, J. R.; Churchill, M. R.; Bueno, C.; Rheingold, A. L. *J. Am. Chem. Soc.* **1982**, *104*, 7347. (b) Churchill, M. R.; Bueno, C.; Rheingold, A. L. *J. Organomet. Chem.* **1990**, *395*, 85.

S0276-7333(98)00565-2 CCC: $15.00
Publication on Web 08/19/1998

Scheme 1

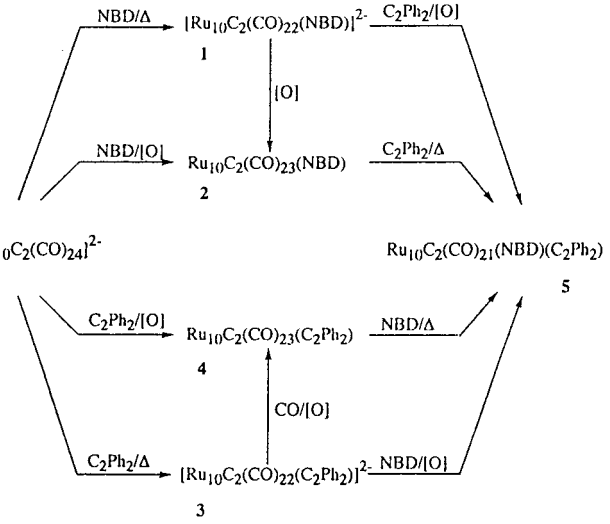

"inner" site at or near the area of fusion, which contrasts with the typical type of "outer" site on the convex surface of the cluster frame. We have shown that $[Ru_{10}C_2(CO)_{24}]^{2-}$ undergoes thermal substitution at ca. 125 °C with diphenylacetylene or allene to form the derivatives $[Ru_{10}C_2(CO)_{22}(C_2Ph_2)]^{2-}$ [7a] or $[Ru_{10}C_2(CO)_{22}(C_3H_4)]^{2-}$,[7b] respectively, and that under a carbon monoxide atmosphere at 125 °C these compounds transform back to $[Ru_{10}C_2(CO)_{24}]^{2-}$. These reversible thermal substitutions demonstrate the robust character of the $Ru_{10}C_2$ framework, which contrasts with that of the monocarbido decaruthenium cluster $[Ru_{10}C(CO)_{24}]^{2-}$, since the latter compound was observed to degrade to $[Ru_6C(CO)_{16}]^{2-}$ and $Ru_3(CO)_{12}$ upon exposure to carbon monoxide (1 atm) at room temperature.[8] We have also previously shown that $[Ru_{10}C_2(CO)_{24}]^{2-}$ can undergo oxidative substitution with diphenylacetylene and ferrocenium to form a neutral alkyne derivative $Ru_{10}C_2(CO)_{23}(C_2Ph_2)$.[9] In both alkyne-substituted $Ru_{10}C_2$ compounds, the alkyne ligand is in an "inner" position bridging an apical Ru−Ru bond with a μ-η^2, η^2 bonding mode.

In this paper we show that $[Ru_{10}C_2(CO)_{24}]^{2-}$ can also undergo thermal substitution with a different four-electron donor ligand, namely, norbornadiene (NBD), to afford $[Ru_{10}C_2(CO)_{22}(NBD)]^{2-}$. Oxidation of $[Ru_{10}C_2(CO)_{22}(NBD)]^{2-}$ in the absence of added ligands forms $Ru_{10}C_2(CO)_{23}(NBD)$, which we have prepared also from the oxidative substitution of $[PPN]_2[Ru_{10}C_2(CO)_{24}]$ with NBD. In both compounds, the NBD ligand is in an "outer" position, on an equatorial ruthenium. We also prepared a doubly substituted product $Ru_{10}C_2(CO)_{21}(NBD)(C_2R_2)$ (R = Ph, Tol) in four distinct ways by utilizing both thermal substitution and oxidative substitution (see Scheme 1). The substitution site specificity of the metal framework is substantiated by showing that the NBD ligand is in an "outer" position coordinating one equatorial ruthenium and the alkyne ligand in an "inner" position bridging an apical Ru−Ru bond. We describe the preparation and characterization of these compounds, supported in part by X-ray diffraction studies of $Ru_{10}C_2(CO)_{23}(NBD)$ and $Ru_{10}C_2(CO)_{21}(NBD)(C_2Ph_2)$.

Experimental Section

Materials and Methods. All reactions were carried out under a nitrogen atmosphere by using standard inert atmosphere techniques.[10] The reaction solvents were reagent grade and were dried over appropriate drying agents and distilled immediately before use. $[Cp_2Fe][BF_4]$[11] and C_2Tol_2[12] were prepared according to the literature. $[PPN]_2[Ru_{10}C_2(CO)_{24}]$ was prepared according to the literature procedure[6] as modified by Ma.[13] The reagents diphenylacetylene (Aldrich), carbon monoxide (MG Industries), and bicyclo[2.2.1]hepta-2,5-diene (NBD, Aldrich) were used as received. IR spectra were recorded on a Perkin-Elmer 1750 FT-IR spectrometer. ^{1}H NMR spectra were recorded on General Electric QE 300 and Varian Unity 400 spectrometers. X-ray diffraction data, negative-ion fast atom bombardment mass spectra, and elemental analyses were provided by the staff of the Materials Chemistry Laboratory, the Mass Spectrometry Center, and the Microanalytical Laboratory of the School of Chemical Sciences, respectively.

Preparation of $[PPN]_2[Ru_{10}C_2(CO)_{22}(NBD)]$ (1). A diglyme (20 mL) solution of $[PPN]_2[Ru_{10}C_2(CO)_{24}]$ (62.0 mg, 0.0223 mmol) was prepared in a 50 mL three-necked flask equipped with a reflux condenser. The ligand NBD (3 mL, 28 mmol) was introduced via a syringe, and then the solution was heated to 140 °C. After ca. 2 h, no IR peaks corresponding to the starting material were observed. The solvent was removed under vacuum at an ambient temperature, the dark residue was dissolved in dichloromethane, and the products were separated by TLC (silica gel, dichloromethane/hexane/acetone, 3:1:1). The major product **1** appeared at low R_f as a red-purple band, which was extracted with acetone and isolated as a purple solid (25.4 mg, 0.0090 mmol, 40%). Anal. Calcd for $C_{103}H_{68}O_{22}N_2P_4Ru_{10}$: C, 43.87; H, 2.43; N, 0.99. Found: C, 43.20; H, 2.21; N, 0.85. FAB(−) mass spectrum (^{102}Ru): m/z 1751 ($[Ru_{10}C_2(CO)_{22}(C_7H_8)]^-$) as well as 1751 − 28$x$, x = 1−13. IR(CH_2Cl_2): ν_{CO}, 2060 (vw), 2039 (w), 2016 (m, sh), 1997 (vs) cm^{-1}. ^{1}H NMR (CD_2Cl_2, 0 °C): δ 7.68−7.44 (m, 60H, C_6H_5), 4.04 (s(br), 1H, CH), 3.87 (s(br), 1H, CH), 3.82 (s, 2H, =CH), 3.32 (s(br), 1H, =CH), 2.99 (s(br), 1H, =CH), 1.34 (d, 1H$_a$, CH_aH_b, $J(H_aH_b)$ = 9.0 Hz), 1.18 (d, 1H$_b$).

Preparation of $Ru_{10}C_2(CO)_{23}(NBD)$ (2). (A) By Oxidation of 1. A dichloromethane (20 mL) solution of **1** (18.2 mg, 0.0065 mmol) was prepared in a 50 mL Schlenk tube connected to a bubbler. Solid $[Cp_2Fe][BF_4]$ (15.0 mg, 0.055 mmol) was added against a nitrogen stream, and the resulting solution was heated to reflux. After 0.5 h, no IR peaks corresponding to the starting material were observed. The solvent was removed under vacuum, and the resulting dark residue was dissolved in dichloromethane and separated by TLC (SiO_2) with dichloromethane/hexane (1:1). Compound **2** was extracted from a major green band and crystallized from dichloromethane by diffusion of hexane at room temperature (3.7 mg, 0.0021 mmol, 32%). Anal. Calcd for $C_{32}H_8O_{23}Ru_{10}$: C, 21.70; H, 0.46. Found: C, 21.37; H, 0.68. FAB(−) mass spectrum (^{102}Ru): m/z 1779 ($[Ru_{10}C_2(CO)_{23}(C_7H_8)]^-$). IR($CH_2Cl_2$): ν_{CO}, 2093 (w), 2070 (m), 2046 (s) cm^{-1}. ^{1}H NMR

(7) (a) Ma, L.; Rodgers, D. P. S.; Wilson, S. R.; Shapley, J. R. *Inorg. Chem.* **1991**, *30*, 3591. (b) Lee, K.; Shapley, J. R. *Organometallics* **1998**, *17*, 4030.
(8) Coston, T.; Lewis, J.; Wilkinson, D.; Johnson, B. F. G. *J. Organomet. Chem.* **1991**, *407*, C13.
(9) Benson, J. W.; Ishida, T.; Lee, K.; Wilson, S. R.; Shapley, J. R. *Organometallics* **1997**, *16*, 4929.
(10) Shriver, D. F.; Drezdzon, M. A. *The Manipulation of Air-Sensitive Compounds*, 2nd ed.; Wiley: New York, 1986.
(11) Hendrickson, D. N.; Sohn, Y. S.; Gray, H. B. *Inorg. Chem.* **1971**, *10*, 1559.
(12) Cope, A. C.; Smith, D. S.; Cotter, R. J.; Price, C. C.; McKeon, T. F., Jr. *Organic Syntheses*; Wiley: New York, 1963; Coll. Vol. IV, p 377.
(13) Ma, L. Ph.D. Thesis, University of Illinois, 1991.

(CD_2Cl_2, 20 °C): δ 4.34 (s(br), 2H, CH), 4.15 (s, 2H, =CH), 3.58 (s(br), 2H, =CH), 1.60 (s(br), 2H, CH_2).

(B) By Oxidative Substitution. A dichloromethane (20 mL) solution of $[PPN]_2[Ru_{10}C_2(CO)_{24}]$ (29.1 mg, 0.0105 mmol) was prepared in a 50 mL Schlenk tube connected to a bubbler. The ligand NBD (0.5 mL, 4.6 mmol) was introduced via syringe. Solid $[Cp_2Fe][BF_4]$ (10.0 mg, 0.0366 mmol) was added against a nitrogen stream, and the solution color immediately changed from purple to green. After 5 min, the IR peaks at 2093 (w), 2070 (m), and 2046 (s) cm^{-1} for **2** were observed. The solvent was removed under vacuum, and the resulting dark residue was purified as above to obtain **2** (4.8 mg, 0.0027 mmol, 26%).

Preparation of $Ru_{10}C_2(CO)_{21}(NBD)(C_2Ph_2)$ (5). (A) From Thermal Substitution of $Ru_{10}C_2(CO)_{23}(C_2Ph_2)$ (4). A dichloromethane (20 mL) solution of $[PPN]_2[Ru_{10}C_2(CO)_{24}]$ (19.0 mg, 0.0068 mmol) and C_2Ph_2 (5.0 mg, 0.028 mmol) was prepared in a 50 mL Schlenk tube. Solid $[Cp_2Fe][BF_4]$ (6.0 mg, 0.022 mmol) was added against a nitrogen stream. After 5 min, the IR spectrum indicated that the reaction was complete to form **4**.[9] The solution was filtered through a short silica gel column (5 cm height) into a 50 mL three-neck flask equipped with a reflux condenser. The solvent was removed under vacuum, and the resulting solid was washed with hexane (ca. 20 mL) to remove ferrocene. Dry toluene (20 mL) and NBD (0.5 mL, 4.6 mmol) were introduced to the flask, and the resulting solution was heated to reflux. The solution color quickly changed from brown to purplish brown, and after 5 min, no compound **4** was detected in the IR spectrum. The solvent was removed under vacuum, and the resulting residue was separated by TLC with dichloromethane/hexane (1:1) to give a purplish brown band of **5**. Dark microcrystals (3.0 mg, 0.0016 mmol, 23%) were obtained from dichloromethane by diffusion of hexane at room temperature. Anal. Calcd for $C_{32}H_8O_{23}Ru_{10}$: C, 27.91; H, 0.96. Found: C, 27.88; H, 1.12. FAB(−) mass spectrum (^{102}Ru): m/z 1901 ($[Ru_{10}C_2(CO)_{21}(C_7H_8)(C_2Ph_2)]^-$) as well as 1901 − 28$x$, x = 1−2. IR(CH_2Cl_2): ν_{CO}, 2086 (m), 2056 (s, sh), 2049 (vs), 2034 (s), 2017 (m, sh) cm^{-1}. ^{1}H NMR (CD_2Cl_2, 20 °C): δ 7.53−7.42 (m, 10H, C_6H_5), 4.26 (m, 1H, CH), 4.04 (m, 1H, =CH), 3.99 (m, 1H, CH), 3.83 (m, 1H, =CH), 3.47 (m, 1H, =CH), 3.03 (m, 1H, =CH), 1.55 (d, 1H_a, CH_aH_b, $J(H_aH_b)$ = 9.9 Hz), 1.51 (d, 1H_b).

(B) From Thermal Substitution of 2. A toluene (20 mL) solution of **2** (11.2 mg, 0.0063 mmol) and C_2Ph_2 (10 mg, 0.056 mmol) was prepared in a 50 mL three-necked flask equipped with a reflux condenser. The resulting solution was heated to reflux. The solution color quickly changed from green to purplish brown, and after 5 min, no starting material was detected by IR spectrum. The solvent was removed under vacuum. Workup as before gave dark crystals of **5** (10.5 mg, 0.0055 mmol, 88%).

(C) From Oxidative Substitution of $[PPN]_2[Ru_{10}C_2(CO)_{22}(C_2Ph_2)]$ (3). A dichloromethane (20 mL) solution of **3** (18.2 mg, 0.0063 mmol) was prepared in a 50 mL Schlenk flask connected to a bubbler. The ligand NBD (0.5 mL, 4.6 mmol) was added via a syringe. Solid $[Cp_2Fe][BF_4]$ (5.0 mg, 0.0183 mmol) was added against the nitrogen stream, and the solution was stirred for 5 min. Workup as before gave dark crystals of **5** (5.2 mg, 0.0027 mmol, 44%).

(D) From Oxidative Substitution of 1. A dichloromethane (20 mL) solution of **1** (62.0 mg, 0.0220 mmol) and C_2Ph_2 (10 mg, 0.13 mmol) was prepared in a 50 mL Schlenk flask connected to a bubbler. $[Cp_2Fe][BF_4]$ (20.0 mg, 0.0733 mmol) was added as a solid against a nitrogen stream, and the solution was stirred for 5 min. The solvent was removed under vacuum, and the resulting residue was separated by TLC with dichloromethane/hexane (1:1) to give a purple-brown band of **5** (8.2 mg, 0.0043 mmol, 20%) and a closely following green band containing **2** (7.5 mg, 0.0042 mmol, 19%).

X-ray Crystallographic Study of 2 and 5. Crystals of **2** and **5** were grown by solvent diffusion of hexane into the respective dichloromethane solutions at room temperature. The data crystals were mounted with oil to thin glass fibers. Data collections were carried out on an Enraf-Nonius CAD4 diffractometer for **2** and on a Siemens SMART/CCD diffractometer for **5**. The data crystal for **5** exhibited rather weak diffraction. A summary of crystallographic data is given in Table 1, and more complete details are presented in the Supporting Information.

Table 1. Crystallographic Data for $Ru_{10}C_2(CO)_{23}$(NBD) (2) and $Ru_{10}C_2(CO)_{21}(NBD)(C_2Ph_2)\cdot 0.5CH_2Cl_2$ (5·0.5CH_2Cl_2)

	2	**5**·0.5CH_2Cl_2
formula	$C_{32}H_8O_{23}Ru_{10}$	$C_{44.5}H_{19}ClO_{21}Ru_{10}$
fw	1771.08	1935.75
space group	$P\bar{1}$	$P2_1/c$
cryst syst	triclinic	monoclinic
a (Å)	10.067(6)	19.448(8)
b (Å)	12.206(4)	13.208(5)
c (Å)	19.231(5)	20.203(9)
α (deg)	71.68(2)	90
β (deg)	79.39(3)	106.55(1)
γ (deg)	65.86(3)	90
V (Å^3)	2043(2)	4975(4)
Z	2	4
temp (K)	198(2)	198(2)
λ(Mo Kα) (Å)	0.710 73	0.710 73
cryst size (mm^3)	0.15 × 0.15 × 0.03	0.02 × 0.06 × 0.08
ρ_{calc} (g·cm^{-3})	2.879	2.585
μ(Mo Kα) (mm^{-1})	3.673	3.078
trans coeff, max/min	0.899/0.590	0.940/0.748
abs corr	integration	integration
no. of reflns collected	6065	14003
no. of indep reflns	5679	4007
R_{int}	0.0362	0.2798
$R(F_o)^a$ [$I > 2\sigma(I)$]	0.0334	0.0805
$R_w(F_o^2)^b$	0.0732	0.1354

^{a} $R(F_o) = \sum||F_o| - |F_c||/\sum|F_o|$. ^{b} $R_w(F_o^2) = \{\sum[w(F_o^2 - F_c^2)^2]/\sum w(F_o^2)^2]\}^{1/2}$.

All data processing was performed with the integrated program package SHELXTL.[14] The structures were solved by direct methods;[15] positions for the ruthenium atoms were deduced from an E map. One cycle of isotropic least-squares refinement followed by an unweighted difference Fourier synthesis revealed positions for the ruthenium and remaining non-hydrogen atoms. Hydrogen atoms were not included in the final structure factor calculations. All non-hydrogen atoms were refined with anisotropic thermal coefficients for **2**, and only ruthenium atoms were refined with anisotropic thermal coefficients for **5**. Successful convergences of full-matrix least-squares refinement on F^2 in both cases were indicated by the maximum shift/error for the final cycle. The final difference Fourier maps had no significant features. The Ru−Ru distances for **2** and **5** are listed in Table 2.

Results and Discussion

Synthesis and Characterization of 1, 2, and 5. Substitution of carbonyl ligands in $[PPN]_2[Ru_{10}C_2(CO)_{24}]$ by NBD in diglyme at 140 °C followed by separation of the reaction mixture on a silica gel TLC plate afforded red-purple $[PPN]_2[Ru_{10}C_2(CO)_{22}(NBD)]$ (**1**) in 40% yield. The negative-ion FAB mass spectrum of **1** showed the isotope multiplet pattern for the ion corresponding to $[Ru_{10}C_2(CO)_{22}(NBD)]^-$ (m/z = 1751) as well as ion multiplets with a difference of one to 13 carbonyl ligands.

(14) Sheldrick, G. M. *SHELXTL PC, Version 5.0*; Siemens Industrial Automation, Inc.: Madison, WI, 1994.
(15) Sheldrick, G. M. *Acta Crystallogr.* **1990**, *A46*, 467.

Table 2. Ru−Ru Distances (Å) for $Ru_{10}C_2(CO)_{23}$(NBD) (2) and $Ru_{10}C_2(CO)_{21}$(NBD)(C_2Ph_2) (5)

	2	5
	Apical−Equatorial	
Ru1−Ru3	2.802(1)	2.762(6)
Ru2−Ru4	2.764(2)	2.830(6)
Ru5−Ru6	2.790(2)	2.869(6)
Ru6−Ru8	2.788(2)	2.875(6)
Ru1−Ru2	2.826(2)	2.978(6)
Ru3−Ru4	3.022(2)	2.895(5)
Ru5−Ru7	2.914(1)	2.816(5)
Ru7−Ru8	2.873(2)	2.759(6)
	Apical−Hinge	
Ru1−Ru9	3.022(1)	3.005(5)
Ru8−Ru9	2.862(2)	2.931(5)
Ru8−Ru10	2.958(1)	2.917(5)
Ru1−Ru10	2.841(2)	2.892(5)
Ru4−Ru9	2.865(1)	3.036(5)
Ru5−Ru9	3.304(2)	3.023(5)
Ru5−Ru10	2.882(1)	3.272(5)
Ru4−Ru10	3.424(2)	2.975(6)
	Hinge−Hinge	
Ru9−Ru10	2.789(2)	2.791(5)
	Equatorial−Hinge	
Ru2−Ru9	2.896(1)	2.944(5)
Ru3−Ru10	3.206(1)	2.932(6)
Ru6−Ru10	2.921(1)	2.853(5)
Ru7−Ru9	2.857(1)	2.902(5)
	Equatorial−Equatorial	
Ru2−Ru3	2.980(2)	3.000(6)
Ru6−Ru7	3.015(2)	3.050(6)
	Apical−Apical	
Ru4−Ru5	2.939(2)	2.748(5)
Ru1···Ru8	3.876(2)	3.839(5)

The neutral derivative $Ru_{10}C_2(CO)_{23}$(NBD) (**2**) was prepared in comparable yields either by oxidative substitution of $[PPN]_2[Ru_{10}C_2(CO)_{24}]$ with NBD and ferrocenium or from oxidation of **1** by ferrocenium in the absence of added ligands (26% and 32%, respectively). This green compound was isolated by TLC, and its negative-ion FAB mass spectrum showed the isotope multiplet pattern for the molecular ion $[Ru_{10}C_2(CO)_{23}(NBD)]^-$ (m/z = 1779).

The additional carbonyl ligand in **2** generated by the oxidation of **1** apparently originated from self-scavenging by electron-deficient intermediates, such as $Ru_{10}C_2(CO)_{22}$(NBD) or $[Ru_{10}C_2(CO)_{22}(NBD)]^{1-}$, as was observed in the formation of $Ru_6C(CO)_{17}$ from $[Ru_6C(CO)_{16}]^{2-}$.[16] Treatment of **1** with $[Cp_2Fe][BF_4]$ in the presence of carbon monoxide (1 atm) produced only an unstable brown neutral compound (IR: ν_{CO}, 2075 (s), 2055 (vs) cm^{-1}), which did not transform to **2** upon heating or standing at room temperature. However, oxidation of **1** with $[Cp_2Fe][BF_4]$ at lower carbon monoxide concentration (0.01 atm) did not form either **2** or this brown compound. Thus, the formation of **2** is apparently inhibited by the presence of carbon monoxide, which can divert the reaction in other directions.

When **1** was oxidized by 2 equiv of $[Cp_2Fe][BF_4]$ in the presence of excess C_2Ph_2, the ν_{CO} region of the IR spectrum of the reaction mixture showed a completely new set of peaks in 5 min with a color change from red-purple to purplish brown. Subsequent separation by TLC afforded red-purple $Ru_{10}C_2(CO)_{21}$(NBD)(C_2Ph_2) (**5**) in 19% yield. The negative-ion FAB mass spectrum of **5** showed the isotope multiplet pattern for the molecular ion $[Ru_{10}C_2(CO)_{21}(NBD)(C_2Ph_2)]^-$ (m/z = 1901) as well as ion multiplets differing in mass by one or two carbonyl ligands. Compound **5** can also be prepared by other methods (see Scheme 1) in generally higher yields: by substitution of two carbonyl ligands in **2** by C_2Ph_2 in refluxing toluene (88%); by oxidation of $[PPN]_2[Ru_{10}C_2(CO)_{22}(C_2Ph_2)]$ (**3**) with $2[Cp_2Fe][BF_4]$ in the presence of NBD (44%); and by substitution of two carbonyl ligands in $Ru_{10}C_2(CO)_{23}(C_2Ph_2)$ (**4**) by NBD in refluxing toluene (23%).

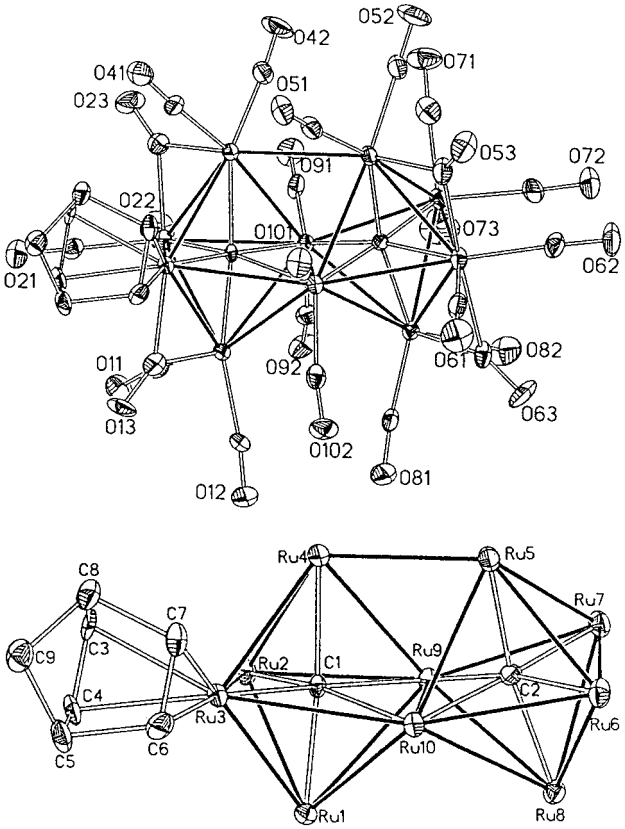

Figure 1. Structural diagrams for $Ru_{10}C_2(CO)_{23}$(NBD) (**2**) (35% thermal ellipsoids). Top: entire molecule with carbonyl oxygen atoms labeled. Bottom: $Ru_{10}C_2$ framework and ligand labeling.

X-ray Crystallographic Study of 2 and 5. The structural diagrams of **2** and **5** are shown in Figure 1 and Figure 2, respectively. Categories of metal−metal distances in the structures of **2** and **5** are presented in Table 2.

The overall geometry of the 10 ruthenium atoms and two interior carbon atoms constituting the framework of **2** is derived from the edge-shared, carbide-centered bioctahedral framework displayed by the parent compound $[Ru_{10}C_2(CO)_{24}]^{2-}$,[6] but with significant distortions in various metal−metal distances. In comparison with the apical−apical Ru−Ru distances in the parent (average 3.130 Å), the corresponding distances for **2** are both shorter (Ru4−Ru5 = 2.939(2) Å) and longer (Ru1···Ru8 = 3.876(2) Å). Furthermore, there is a significant twist of the two octahedral subunits in opposite directions about the hinge bond (Ru9−Ru10) that joins them, which results in significant elongation in the apical−hinge distances Ru4−Ru10 = 3.424(2) Å and Ru5−Ru9 = 3.304(2) Å. The NBD ligand binds to an "outer"

(16) Drake, S. R.; Johnson, B. F. G.; Lewis, J. *J. Chem. Soc., Dalton Trans.* **1989**, 243.

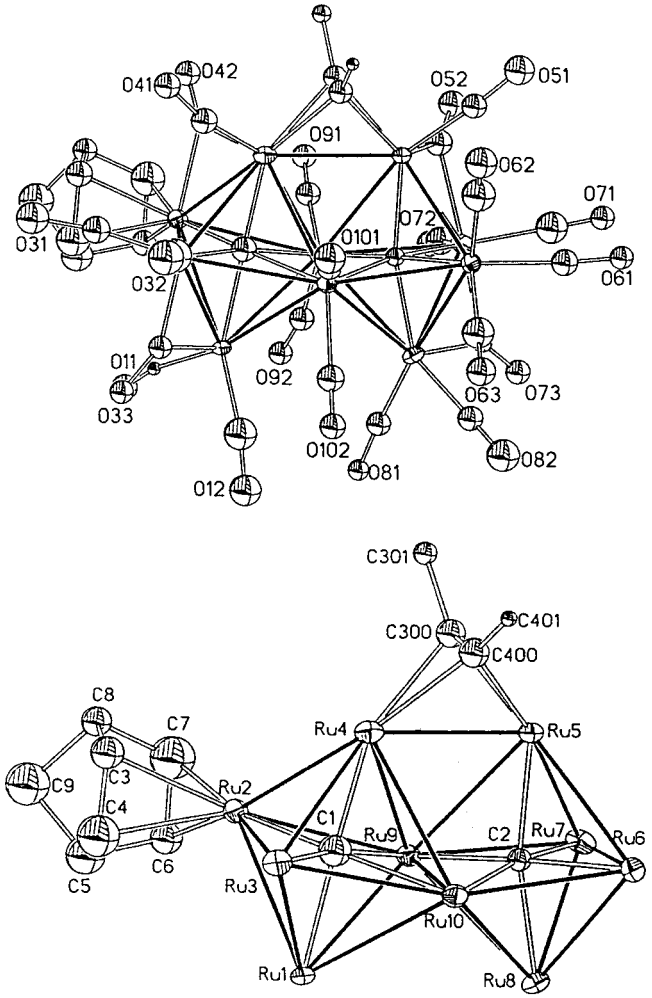

Figure 2. Structural diagrams for $Ru_{10}C_2(CO)_{21}(NBD)(C_2Ph_2)$ (**5**) (35% thermal ellipsoids). Top: entire molecule (except ipso carbons only for phenyl rings), with carbonyl oxygen atoms labeled. Bottom: $Ru_{10}C_2$ framework and ligand labeling.

position at Ru3 in the chelating η^2, η^2 mode. The four bridging carbonyls appear along the Ru1−Ru3, Ru2−Ru4, Ru5−Ru6, and Ru6−Ru8 edges. This unsymmetrical distribution of bridging carbonyl ligands is in contrast to the symmetrical distribution seen for the parent dianion[6] and for the anionic derivatives **3** and $[Ru_{10}C_2(CO)_{22}(C_3H_4)]^{2-}$.[7b] However, an analogous unsymmetrical distribution is seen for the neutral derivatives **4**[9] and **5** (see below). Also, the distance (1.95(1) Å) between Ru3 and the neighboring carbide C1 is much shorter than the other Ru−carbide distances (av 2.08 Å).

The overall geometry of the 10 ruthenium atoms of **5** is again based on edge-shared octahedra. There are four bridging carbonyls distributed unsymmetrically along the Ru1−Ru3, Ru2−Ru4, Ru5−Ru7, and Ru7−Ru8 edges. The NBD ligand binds to equatorial ruthenium atom Ru2 in the η^2, η^2 mode, and the diphenylacetylene ligand bridges apical ruthenium atoms Ru4 and Ru5 in the μ-η^2, η^2 mode. Formally, **5** can be viewed as the substitution product either of **2**, after replacing two terminal carbonyls on adjacent apical ruthenium centers by C_2Ph_2, or of **4**, after replacing two terminal carbonyls on one equatorial ruthenium by NBD (see Scheme 1). The alkyne-bridged Ru4−Ru5 distance of 2.748(5) Å in **5** is comparable to the corresponding apical Ru−Ru distances of 2.738(2) Å in **4**[9] and 2.711(1) Å in **3**,[7a] and it is significantly shorter than the nonbridged apical Ru−Ru distance of 2.939(2) Å in **2**. Overall, the distribution of Ru−Ru distances in the cluster framework of **5** is more similar to that of **4**[9] than to that of **2**. However, as in **2** the distance (1.95(4) Å) between NBD-bound Ru2 and carbide C1 is markedly shorter than the other Ru−carbide distances (average 2.08(4) Å).

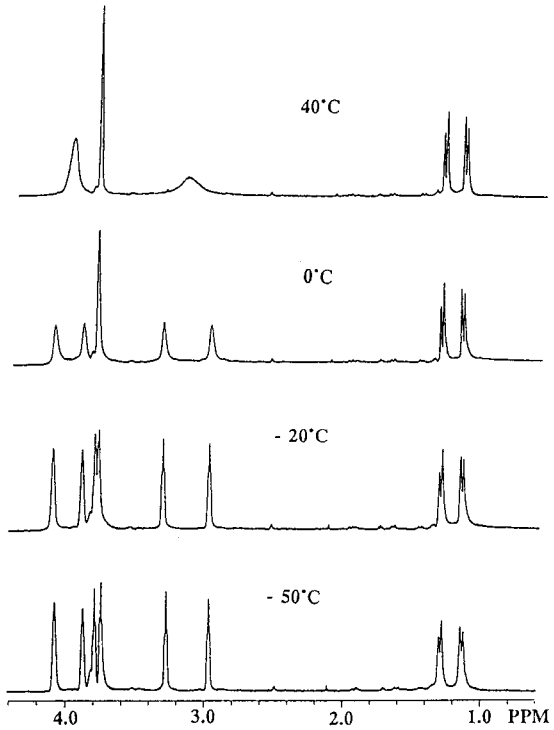

Figure 3. ^{1}H NMR spectra of $[PPN]_2[Ru_{10}C_2(CO)_{22}(NBD)]$ (**1**) in CD_2Cl_2 at selected temperatures.

Scheme 2

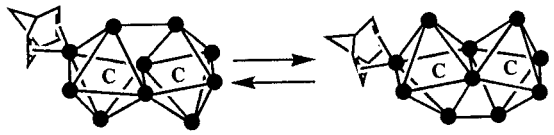

^{1}H NMR spectra of 1, 2, and 5. The ^{1}H NMR spectrum of **1** at −50 °C exhibits eight equally intense signals for the NBD ligand (Figure 3). The two doublets at δ 1.34 and 1.18 are assigned to the two methylene hydrogens, the two broad singlets at δ 4.04 and 3.97 are assigned to the two bridgehead hydrogens, and the four multiplets between are assigned to the four vinylic hydrogens. This pattern is consistent with our assumption that the NBD ligand in **1** is chelating an equatorial ruthenium as shown in the solid-state structures of **2** and **5**. At higher temperatures, the signals in the downfield region coalesce in three pairs, whereas the two methylene hydrogen signals do not change (Figure 3). It is clear that **1** is fluxional in solution and undergoes a rearrangement that equilibrates the two bridgehead positions and hence the two hydrogens on each double bond of the NBD ligand. We propose that this behavior results from reversible Ru−Ru bond making and breaking in the $Ru_{10}C_2$ framework as shown in Scheme 2. This top/bottom interchange of pairs of

apical positions would generate an effective mirror plane containing all the equatorial Ru atoms.

The ^{1}H NMR spectrum of **2** at room temperature exhibits four equally intense signals for the NBD ligand. The pattern is similar to that for the signals of **1** at ca. 40 °C, and by comparing the signal patterns and peak positions, the broad singlet at δ 4.34 is assigned to bridgehead hydrogens, the sharp singlet at δ 4.15 and the broad feature at δ 3.58 are assigned to vinylic hydrogens, and the broad singlet at δ 1.60 is assigned to methylene hydrogens. This spectrum suggests the presence of a mirror plane containing the methylene hydrogens and bisecting the two double bonds in the NBD, which is inconsistent with the complete lack of symmetry shown in the solid-state structure of **2**. Thus, it is tempting to suggest that a process analogous to that shown in Scheme 2 is operating for compound **2** as well. Unfortunately, the solubility of **2** is much less than that of **1**, and we were unable to obtain appropriate low-temperature spectra to characterize this behavior.

The ^{1}H NMR spectrum of compound **5** at room temperature shows eight equally intense signals for the NBD ligand, which is consistent with the lack of symmetry in the solid-state structure. Two broad singlets at δ 4.26 and 3.99 are assigned to the bridgehead hydrogens, four pseudotriplets at δ 4.04, 3.83, 3.47, and 3.03 are assigned to the vinylic hydrogens, and two doublets at δ 1.55 and 1.51 are assigned to the methylene hydrogens. No change in the spectrum was observed at higher temperatures. Thus, there is no fluxional behavior for **5** that equilibrates positions in the NBD ligand, and it is clear that coordination of the alkyne ligand in the "inner" position must severely limit the possibilities for rearrangement of the $Ru_{10}C_2$ framework.

Site Selectivity of Ligand Substitution. The parent compound $[Ru_{10}C_2(CO)_{24}]^{2-}$ reacts thermally with NBD to give **1** and is oxidatively substituted with NBD in the presence of ferrocenium to afford **2**. In both **1** and **2** the NBD ligand is in an "outer" position on an equatorial ruthenium of the $Ru_{10}C_2$ framework. On the other hand, in the alkyne ligand derivatives **3**, **4**, and **5**, the alkyne ligand is located in an "inner" position of the $Ru_{10}C_2$ framework, bridging an apical Ru−Ru vector with a μ-η^2, η^2 bonding mode. The selectivy of these two sites toward the different 4e ligands, NBD and C_2Ph_2, is thoroughly demonstrated in the formation of **5** by four distinct pathways.

These coordination site preferences for the two ligands can be rationalized by considering the ligand geometry and the electronic configuration of the $Ru_{10}C_2$ framework. According to the Wade−Mingos rules,[17] a 10-atom D_{2h} framework formed by two edge-fused octahedra with apical metal−metal bonds would possess a total of 134 valence electrons. In $[Ru_{10}C_2(CO)_{24}]^{2-}$, a total of 138 valence electrons is present, and the elongated apical−apical Ru−Ru distances found in $[Ru_{10}C_2(CO)_{24}]^{2-}$ were attributed to the localization of four extra electrons on the apical Ru−Ru antibonding orbitals, thus *formally* reducing the apical Ru−Ru bond order to zero.[6] The μ-η^2, η^2 configuration of the alkyne ligand in **3**, **4**, and **5** seems to provide the optimal geometry for strong π-back-bonding from the antibonding orbital interactions between the apical metal centers to the alkyne ligand. In forming the complex some of the metal−metal antibonding interaction is stabilized as metal−ligand bonding, resulting in a net increase in the bonding character in the apical Ru−Ru interaction. This is demonstrated by the severe shrinkage of the alkyne-bridged, apical Ru−Ru distance in **3**, **4**, and **5** from that in $[Ru_{10}C_2(CO)_{24}]^{2-}$.[6,7a] The inward pointing π-orbitals of the NBD ligand are not oriented properly to bridge two apical Ru centers, but the NBD ligand could potentially replace two carbonyls and chelate at one apical Ru atom. However, this position would likely increase the destabilizing nonbonded interactions between the apical centers without promoting bonding interactions. The preferred position for this chelating diene ligand, therefore, is to replace two terminal carbonyls at an "outer" position on an equatorial Ru center.

Acknowledgment. This material is based upon work supported by the National Science Foundation under Award No. CHE 9414217. We thank Dr. Scott R. Wilson of the School of Chemical Sciences Materials Chemistry Laboratory for collection of X-ray data. Purchase of the Siemens Platform/CCD diffractometer by the School of Chemical Sciences at the University of Illinois was supported by National Science Foundation Grant CHE 9503145. NMR spectra were obtained using instruments in the Varian Oxford Instrument Center for Excellence in NMR Laboratory in the School of Chemical Sciences; external funding for this instrumentation was obtained from the Keck Foundation, NIH, and NSF.

Supporting Information Available: Tables of positional parameters, bond distances, bond angles, and anisotropic thermal parameters for the structural analyses of compounds **2** and **5**·0.5CH_2Cl_2 (35 pages). See any current masthead page for ordering and Internet access instructions.

OM980565S

(17) Mingos, D. M. P.; Wales, D. J. *Introduction to Cluster Chemistry*; Prentice Hall: Engelwood Cliffs, NJ, 1990.